

## MATHEMATICAL MODELLING OF COLLAGEN FIBRES REARRANGEMENT DURING THE TENDON HEALING PROCESS

JOSÉ ANTONIO CARRILLO

Mathematical Institute, University of Oxford  
Oxford OX2 6GG, United Kingdom

MARTIN PARISOT

Inria-Bordeaux, Team CARDAMOM, Office B426  
200 av. de la vieille tour, 33405 Talence Cedex, Bordeaux, France

ZUZANNA SZYMAŃSKA\*

Institute of Mathematics, Polish Academy of Sciences  
ul. Śniadeckich 8, 00-656 Warsaw, Poland  
ICM, University of Warsaw  
ul. Tyniecka 15/17, 02-630 Warsaw, Poland

(Communicated by Gabriella Puppo)

**ABSTRACT.** Tendon injuries present a clinical challenge to modern medicine as they heal slowly and rarely is there full restoration to healthy tendon structure and mechanical strength. Moreover, the process of healing is not fully elucidated. To improve understanding of tendon function and the healing process, we propose a new model of collagen fibres rearrangement during tendon healing. The model consists of an integro-differential equation describing the dynamics of collagen fibres distribution. We further reduce the model in a suitable asymptotic regime leading to a nonlinear non-local Fokker-Planck type equation for the spatial and orientation distribution of collagen fibre bundles. Due to its simplicity, the reduced model allows for possible parameter estimation based on data. We showcase some of the qualitative properties of this model simulating its long time asymptotic behaviour and the total time for tendon fibres to align in terms of the model parameters. A possible biological interpretation of the numerical experiments performed leads us to the working hypothesis of the importance of tendon cell size in patient recovery.

**1. Introduction.** Tendon injuries, although not directly threatening the lives of affected persons, can significantly lower quality of life [44]. Despite the enormous progress of medicine over the last decades, little has been achieved in improving the treatment of these injuries. A significant research obstacle is the difficulty in setting up a proper experimental environment, as it is generally not possible to biopsy healthy tendon tissues from patients or volunteers [45]. At present most of the injuries are treated by surgical repair and/or conservative approaches such

---

2020 *Mathematics Subject Classification.* Primary: 35R09, 92-08, 92-10; Secondary: 92B05, 92C50.

*Key words and phrases.* Collagen remodelling, Kinetic model, Tendon healing, Integro-differential equations, Alignment.

\* Corresponding author: z.szymanska@icm.edu.pl.

as physical rehabilitation and cryotherapy [53]. The healing tissue tends to form fibrovascular scars and possesses inferior mechanical and biochemical properties as compared to pre-injury tissue [53]. Only recently, with the development of regenerative medicine, have new treatment perspectives emerged. However, their effective implementation requires a thorough understanding of the healing process, which is particularly difficult due to specific tendon morphology and the low cellularity and poor blood supply of tendon tissue. Mathematical modelling may provide additional insight [43].

The modelling of the process of tendon healing has virtually not been addressed in the literature until recently. Some works have analysed equilibrium configurations based on macroscopic elasticity models [1, 2, 3]. However, the dynamics of the tendon healing process, leading to possible modelling of healing time, have not been discussed at all. Moreover, despite sharing a lot of similarities with other types of wound healing, the tendon healing process is beyond the range of applicability of classical wound healing models. The reason is that classical wound healing models do not focus on collagen fibres structure, which in most tissues does not play such an important role as in a tendon. In the case of tendon healing, an adequate description of the reconstruction of the parallel structure of collagen fibres is absolutely essential. Collagen fibres tend to align locally in a similar way as individuals, cells or fibres in other models of alignment. Therefore, perhaps surprising at first glance because the nature of the described phenomena is different, a mathematical description of tendon healing may draw more from kinetic models of alignment or consensus processes such as: reorientation mechanisms for collective behaviour of individuals in fish shoals or flocks of birds [26, 19, 9, 27, 4, 12, 42, 34], polymer models [6, 7, 30], cell movement for chemotaxis [40, 41, 10], opinion formation models [51, 29], migration models [37], and tissue remodelling of extracellular matrix fibres [14].

Only recently a simple model for the dynamics of collagen remodelling occurring in the latter stage of the tendon healing process was proposed by Dudziuk et al. [25]. The authors propose an integro-differential equation describing the dynamics of the probability density of collagen fibres in space and orientation. As usual in kinetic models, they follow a statistical description of the system by the mass distribution of collagen fibres in the tendon tissue. They show that depending on initial data, solutions may either exist globally in time or blow-up in  $L^\infty$ , i.e. concentration in orientation, in a finite time. The latter behaviour can be interpreted as injury healing without scar formation. In the present paper, we build on this statistical description based on fibre bundles orientation by including local alignment interactions between fibres adapted to the modelling of tendon tissue, cf. [12]. The particular structure of these kinetic models allows for the derivation of simplified models for the associated dynamics via the methodology of grazing collision limits, that is, the integro-differential operators is approximated by Fokker-Planck differential operators of second order. This powerful tool of kinetic theory, used in other applications [50, 51, 15], allows for a reduction in the complexity of the kinetic model for the dynamics of tendon healing compared to [25]. In summary, the main contribution of our work is to propose a reduced model for the dynamics of tendon healing compared to previous literature.

Finally, we would like to raise one more issue namely, most of the biophysical models miss a genuine connection to experimental data, which results in the limited

predictive value of these models. Usually, this is due to the difficulty in reliable measurement of parameters. However, this difficulty might be overcome by applying an inverse problem approach, that, despite being a considerable challenge, has already been successfully implemented for some biological models, like size-structured models of cell division with non-local kernels [46, 21, 22, 23, 24]. However, one has to bear in mind that such parameter estimation is commonly very costly in terms of computational resources, especially, if the number of parameters is large. This refers also to the alignment kernels that usually contain many parameters. Therefore, we consider the reduction of the model – which decreases the number of parameters, thereby easing possible parameter estimation – as one of the main achievements of this work.

This paper is structured as follows. First, in Section 2 we discuss the main biological aspects of tendon tissue and the healing process after an injury. In Section 3 we introduce the mathematical model and its associated reduction via an asymptotic limit. Section 4 is devoted to the description of the numerical method used to simulate the reduced model and to present the results of simulations. We also explore the qualitative properties of the reduced mathematical model, and discuss the impact of particular parameters on total healing time. In Section 5 we finish by giving conclusions and suggested direction for future research.

## 2. Biology of the tendon.

**2.1. Tendon structure.** Tendons are regular bands of fibrous connective tissue that connect muscles to bones and enable transmission of forces, thereby ensuring joint movements [52, 54]. They are built of i) various types of collagen and elastin fibres tightly arranged in parallel; ii) a relatively low number of residing tendon cells; and iii) a special, strongly hydrophilic ground substance surrounding cells and fibres which enables the rapid diffusion of water-soluble molecules and cell migration [39, 43]. Collagen and elastin fibres account for 70% and 2% of the dry weight of a tendon, respectively [32]. Type I collagen forms 95% of all tendon collagen and consists of clearly defined, parallel, and wavy bundles essentially aligned longitudinally [35, 39]. Collagen fibres are made from fibrous protein subunits linked together to form long and straight fibres [54]. Aligning the collagen fibres along the long axis of the tendon results in a highly anisotropic tissue, particularly well suited to withstand high uniaxial tensile forces [33, 48]. A healthy tendon is also built to a small extent from elastin and type III collagen [32, 33, 39]. In contrast to type I, type III collagen does not have such a regular, parallel structure and its fibres can be described as rather disorganised.

Tendon tissue is characterised by low cellularity and poor blood supply [17]. About 90% to 95% of the cellular elements of the tendon are tendon-specific fibroblasts, i.e. tenocytes and its immature form, tenoblasts [32, 39]. Tenocytes are spindle-shaped longitudinal cells that lie sparingly in rows between collagen fibrils, whereas more rounded tenoblasts are motile and highly proliferative [39, 43]. Tenocytes and tenoblasts are responsible for producing subunits of collagen fibres, degrading enzymes, and cytokines to maintain the dynamic equilibrium of both the fibrous and non-fibrous components of the tendon [47].

The physiological properties of the tendon are mainly due to its hierarchical structure of increasing collagen complexity: fibrils, fibres (primary bundles), fascicles (secondary bundles), tertiary bundles and the tendon itself [43]. Figure 1 presents the structure of the tendon.

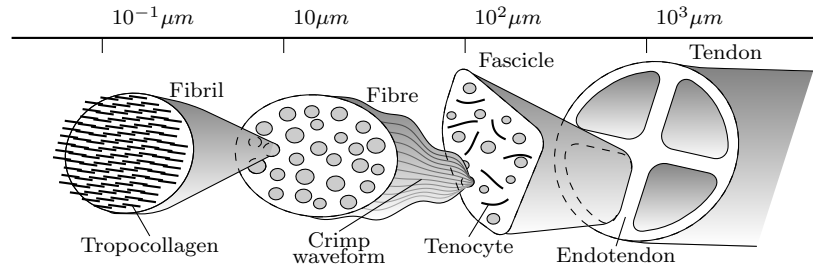


FIGURE 1. Collagen within a tendon has a hierarchical structure of increasing complexity: fibrils, fibres (primary bundles), fascicles (secondary bundles), tertiary bundles and a tendon itself [31, 43].

**2.2. Tendon healing process.** The tendon healing process that follows acute injuries proceeds in stages similar to those taking place in the healing of other connective tissue injuries. It can be divided into three consecutive but overlapping phases: i) inflammatory; ii) proliferative; and iii) remodelling [5, 16, 20, 43, 53].

1. The **inflammatory phase** starts just after the injury. Where vessels have ruptured, the blood clot begins to form. The blood clot induces the release of inflammatory signals that attract and activate inflammatory cells that migrate from surrounding tissue towards the injury [36]. The inflammatory cells phagocytise the necrotic tissue and the clot, initiate the recruitment and activates tendon specific fibroblasts, i.e. tenocytes and tenoblasts [5, 36, 53].

2. The **proliferative phase** begins a few days after the injury [53]. Tendon fibroblasts migrate and proliferate about the injury site where they synthesise components of extracellular matrix - most of the new collagen at this stage is disorganised type III collagen [5, 20, 43, 53], and synthesis of type III collagen peaks during this stage [43].

3. The **remodelling phase** begins roughly 8 weeks after the injury and consists of resizing and reshaping of the healing tissue [43]. It starts with a consolidation sub-stage characterised by the transition of the tissue from cellular to fibrous. Tenocyte metabolism remains high, and collagen fibres become aligned in the direction of stress [53]. The ratio of type I to type III collagen changes in preference to type I [38]. During the maturation sub-stage collagen growth slows down and tenocyte metabolism and tendon vascularity decline [43].

We would like to emphasise that the purpose of our modelling is to deepen the understanding of some phenomena related precisely to the remodelling phase. In particular, we are interested in how collagen fibres align in the direction of the longitudinal axis of the tendon and how disordered type III collagen is transformed into ordered type I collagen. We hypothesise that the mentioned remodelling that is mediated by tenocytes and tenoblasts takes place on the basis of certain self-organisation. The new direction of the fibre is derived at least to some extent from the fibres in the neighbourhood. We propose that tenocytes and tenoblasts, which are relatively large cells, are able to sense the direction of fibres in their close vicinity and change the direction of “non-fitting” fibre to the dominant one. The phenomenon that cells are able to sense direction is known from many biological scenarios, including chemotaxis and haptotaxis. It is known from the clinical practice but also



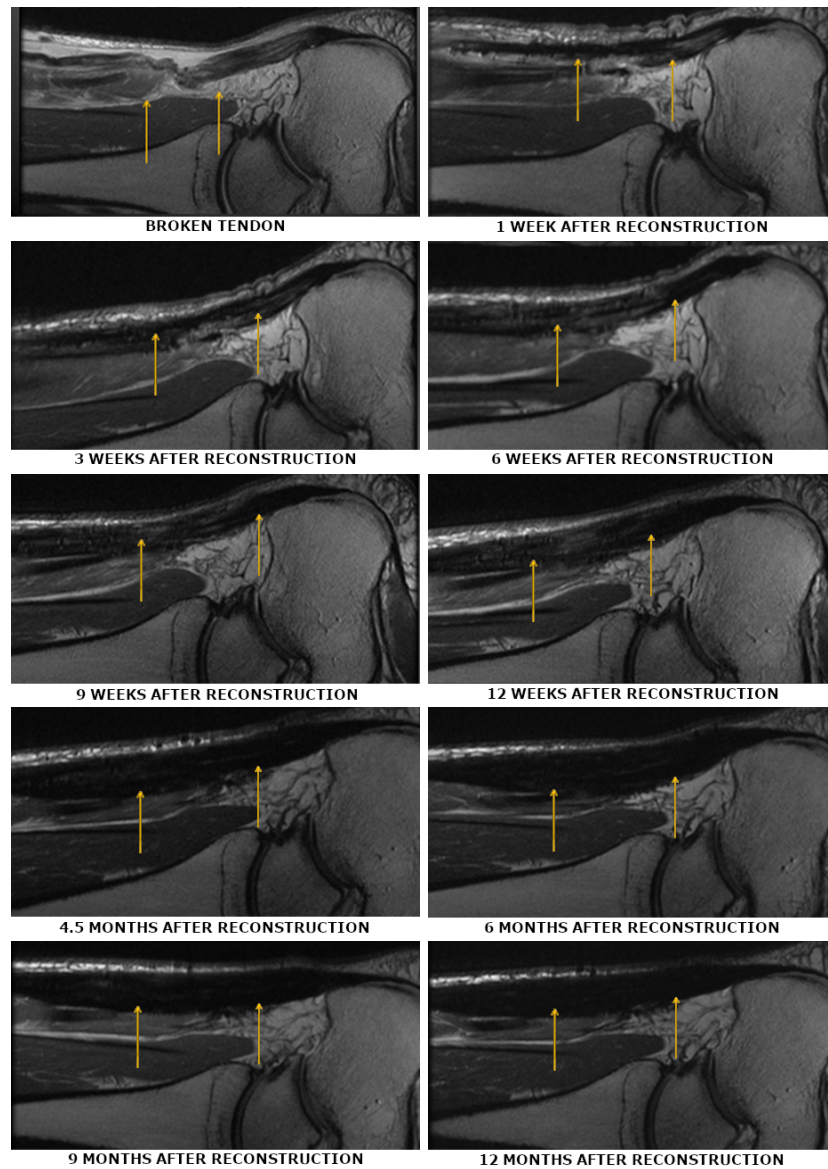


FIGURE 2. Sequence of sagittal sections of a ruptured Achilles tendon taken before the reconstruction and within the first year after the reconstructive surgery. Yellow arrows indicate the tendon.

had some reflection in emerging tendon healing models, see [25], that for the healing process the proper surgical intervention is of the highest importance. “Proper” means the best possible reconstruction of the collagen fibre arrangement along the longitudinal axis. The surgical intervention and the outcome of the following inflammatory and proliferative phases somehow defines the initial conditions of the model. The second important factor is the proper mechanical load that influences the cells making them stretched along the stress. The longer cells are the better

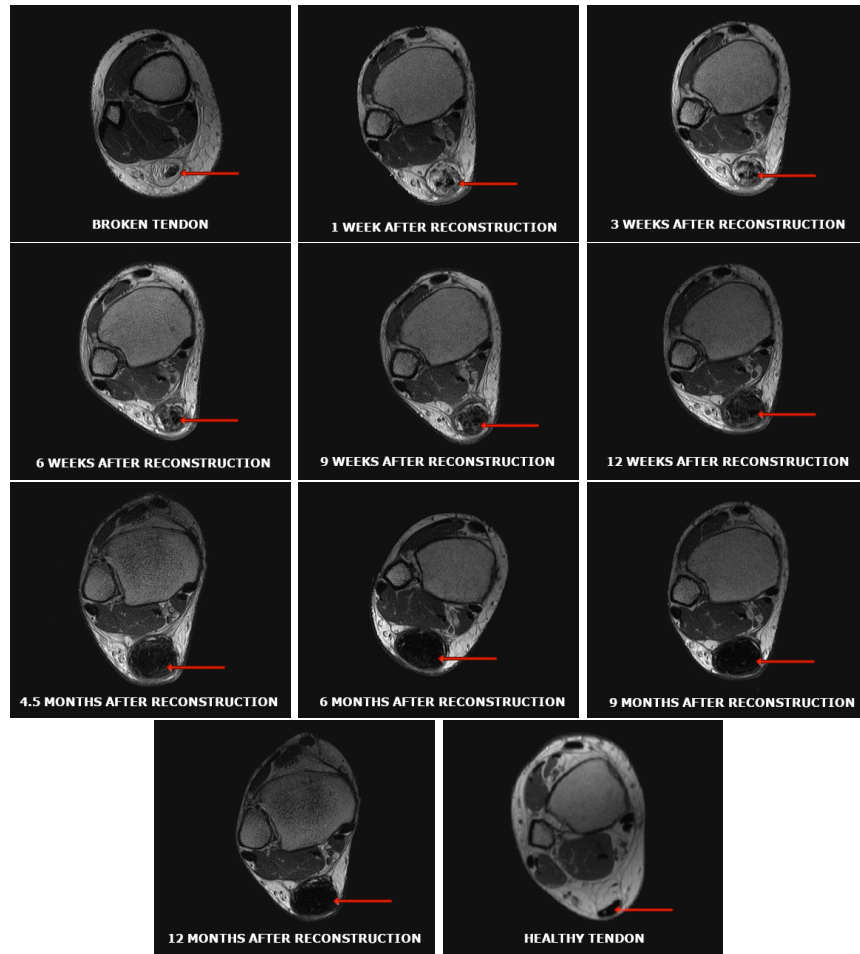


FIGURE 3. Sequence of cross-sections of a ruptured Achilles tendon taken before the reconstruction and within first year after the reconstructive surgery. For comparison, the last image shows the cross-section of a healthy tendon. Red arrows indicate the tendon.

they can sense the dominant direction of surrounding fibres. Let us also mention the new techniques related to regenerative medicine which enable influencing the healing process and which may be captured by different parameters of the model. The new techniques we mean are, for instance, the administration of factors stimulating the metabolism of tendon cells, which results in a more efficient synthesis of collagen fibre building blocks or administration of stem cells, which further differentiate into tenoblasts and then into tenocytes.

Regarding the monitoring of the healing process, few means are currently available. In clinical practice tendon healing is monitored – if at all – by relatively harmless and non-invasive medical imaging technologies such as MRI or ultrasound. Although these methods do not give the full picture as collagen fibres can not be visualised directly, they provide important information on changes in volume and oedema as well as the internal structure of the tendon. The healthy tendon appears

on MRI images as black and internally uniform with no apparent differences. This is mainly related to the proper structure of collagen fibres and very low cellular, water and fat content, i.e. very low amount of hydrogen nuclei that are visible in MRI. The damaged tendon appears much clearer, mostly in grey shades, and internally inhomogeneous. This is mainly because of inflammation, oedema and presence of cells responsible for the healing process.

Figures 2 and 3 present sequences of MRI images monitoring tendon healing process following surgical reconstruction. Within the first weeks, the changes in the MRI are very clear. From about the sixth month or slightly earlier, during the consolidation sub-stage, the changes in the MRI become poorly noticeable. At this time collagen conversion occurs rather than collagen growth. The model we propose approximates exactly this stage of tendon healing.

**3. Mathematical model.** Considering its hierarchical structure we model the tendon as a large collection of fibre bundles. For the sake of clarity, our mathematical description corresponds to the level of the fascicle composed of fibre bundles and rows of tenocytes, cf. Figure 1. The mutual influence of fibres that within the living tissue is mediated by tenocytes, in the model is captured by non-local terms, ipso facto we omit an explicit description of the tenocytes. Moreover, we assume that the fibre bundles are already stretched which allows us to treat them locally as hard sticks where the elasticity properties of the tissue are encoded in the tendency of the local pieces of fibres to align between themselves. The assumption that collagen fibres are already stretched (locally) and therefore can be treated as hard sticks is bolstered by the observation of microscopic images of longitudinal sections of tendons showing the clearly wavy structure of collagen fibres, which indicates that the stretching of the tendon does not come from stretching the collagen fibres themselves, but rather from straightening them. Summarising, we approximate the tendon tissue microscopically by a collection of interacting hard sticks characterised by their orientation, that we denote by  $\phi$ . More precisely,  $\phi$  stands for the acute angle between the tangent of the fibre and the axis of a healthy tendon, see Figure 4.

Although the model can be written in a multi-dimensional framework, in the current study we focus on the one-dimensional case for both position and orientation. As usual in kinetic theory, we do a statistical description of the ensemble of fibres, meaning that position and orientation are independent variables. We are just counting the number of fibres with a given orientation  $\phi$  at a particular position  $x$  modelled by the probability distribution  $f(t, x, \phi)$ . Based on these assumptions, we consider the statistical density function  $f = f(t, x, \phi)$  determining the collagen fibre bundles, i.e. the probability to find a collagen fibre bundle at the instant of time  $t > 0$  at point  $x \in \mathcal{D} \subset \mathbb{R}$  with the orientation angle  $\phi \in [-\frac{\pi}{2}, \frac{\pi}{2}]$ . We propose the following model

$$\begin{aligned} \frac{\partial f}{\partial t}(t, x, \phi) &= Q(f) \quad \text{with collision operator } Q(f) \text{ given by} \\ Q(f) &= \int_{-\frac{\pi}{2}}^{\frac{\pi}{2}} (f(t, x, \phi') T(x, \phi', \phi) - f(t, x, \phi) T(x, \phi, \phi')) d\phi', \end{aligned} \quad (1)$$

where  $T(x, \phi, \phi')$  denotes the turning rate of the collagen fibre bundles at point  $x \in \mathcal{D}$  from orientation  $\phi \in [-\frac{\pi}{2}, \frac{\pi}{2}]$  to orientation  $\phi' \in [-\frac{\pi}{2}, \frac{\pi}{2}]$ . We use the term collision operator for  $Q(f)$  in keeping with the nomenclature adopted in the field of kinetic theory. While this does not model directly biological interactions at the

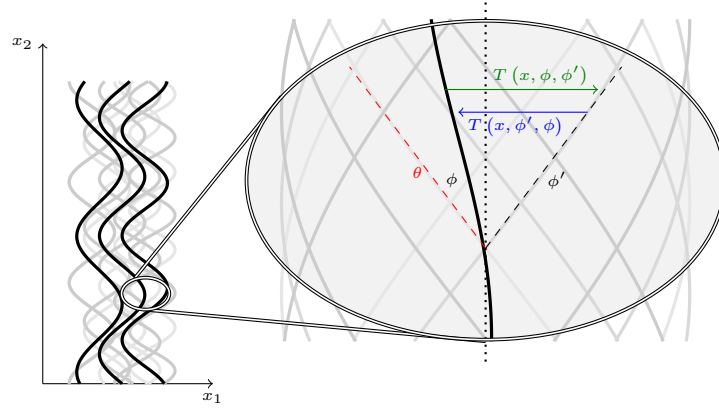


FIGURE 4. Illustration of the connection between mathematical and biological objects. The left side of the image shows a bundle of interacting collagen fibres, whereas the right side shows its magnification at point  $x$ . Turning rate  $T(x, \phi', \phi)$  (blue arrow) models the probability that collagen fibre with orientation  $\phi'$  (black dashed line) rearranges into a fibre with orientation  $\phi$  (solid black line). This turning rate is influenced by all fibres in the neighbourhood whose orientation (example denoted by  $\theta$  and red dashed line) is close enough to  $\phi$ . The reverse action, that is the rearrangement from orientation  $\phi$  to  $\phi'$  obviously exists and is expressed by a green arrow with the  $T(x, \phi, \phi')$  label. The vertical dotted line corresponds to the reference direction  $\phi = 0$ .

microscopic level, it does approximate the fibre dynamics at the mesoscopic level. This operator translates the alignment process which is, as far as we understand, an emerging process of self-reorganisation that incorporates finer mechanics such as elastic interactions or fibre connections. Previously, similar modelling ideas have been used in swarming models [27, 28, 12], kinetic models for chemotaxis [40, 41, 10], and kinetic models for tissue remodelling [14]. Following [27, 12] we define the turning rate as

$$T(x, \phi, \phi') = \int_{\mathcal{D}} \int_{-\frac{\pi}{2}}^{\frac{\pi}{2}} \kappa(x - y) \omega(\phi - \phi', \phi - \theta) \mu[f](t, y, \theta) d\theta dy, \quad (2)$$

where  $\kappa(x)$  and  $\omega(\tilde{\phi}, \tilde{\theta})$  are the space kernel and the orientation kernel, respectively, describing the range of interactions between the fibre bundles. Notice these kernels model the tendency of the fibres to align at the microscopic level due to the interactions mediated by elastic forces in the tissue. Our assumption is that this tendency to align is a local average in space modelled by the localisation kernel  $\kappa(x)$  of the probability of turning orientation modelled by the kernel  $\omega(\tilde{\phi}, \tilde{\theta})$ . The kernels are weighted by  $\mu$ , which is a non-linear function of the density of the fibre bundles defined by

$$\mu[f](t, y, \theta) := \frac{f(t, x, \theta)}{\int_{-\frac{\pi}{2}}^{\frac{\pi}{2}} f(t, x, \theta') d\theta'}.$$

The turning rate  $T(x, \phi, \phi')$  given by (2) averages, with the non-linear weight  $\mu$ , the influence of all fibres in the neighbourhood restricted by both kernels.

Concerning the kernels  $\kappa(x)$  and  $\omega(\tilde{\phi}, \tilde{\theta})$ , we first notice again that the interactions between the fibres are mediated by tenocytes. Relatively large elongated tenocyte size compared to fibre bundles leads us to the assumption that long-range spatial interactions are correlated to cell size, which we model by the support of the localisation in space kernel  $\kappa(x)$ ; see the parameter  $R$  below. The orientation kernel  $\omega(\tilde{\phi}, \tilde{\theta})$  (which is  $\pi$ -periodic with respect to both variables) describes the influence of the orientation of fibre bundles in the neighbourhood. We assume that the change from orientation  $\phi$  to orientation  $\phi'$  arises from interactions with all neighbouring fibre bundles whose orientations are denoted by  $\theta$ . Therefore, the orientation kernel  $\omega(\tilde{\phi}, \tilde{\theta})$  depends on  $\tilde{\phi} = \phi - \phi'$  which is the deviation between original orientation  $\phi$  and orientation to become  $\phi'$  and  $\tilde{\theta} = \phi - \theta$  which is the deviation between original orientation  $\phi$  and any orientation  $\theta$  that causes the change to the orientation  $\phi'$ .

Let us recall some classical kernels that can be found in the literature. The simplest example of the space kernel is given by  $\kappa_0(x) = \kappa_0 \delta(x)$  where  $\delta$  is the delta Dirac function. Other typical examples of spatial and orientation kernels are given by finite distance interactions, that is

$$\kappa_R(x) = \begin{cases} \frac{\kappa_0}{B_R} & |x| \leq R \\ 0 & |x| \geq R \end{cases} \quad \text{and} \quad \omega_\varepsilon(\tilde{\phi}, \tilde{\theta}) = \bar{g}_\varepsilon(\tilde{\phi} - \tilde{\theta}). \quad (3)$$

with

$$\bar{g}_\varepsilon(s) = \begin{cases} \frac{1}{2\varepsilon} & |s| \leq \varepsilon \\ 0 & |s| \geq \varepsilon \end{cases}. \quad (4)$$

Here,  $B_R$  refers to the area of Euclidean ball of radius  $R$  in dimension  $d$ . Other kernels can be a periodised exponential approximation of the Dirac deltas as in [27, subsection 2.2]. The main assumption on the shape of the orientation kernel is that it is localised, which means that the change of orientation is small, as the range parameter  $\varepsilon$  role in (4). In summary, the main parameters of the spatial and the orientation kernels are their range, namely the tenocyte action range  $R$  and the reorientation range  $\varepsilon$ . In the following, we base our model reduction on some assumptions for the kernels (see Hypothesis 1) satisfied by the previous examples. However, the reduction is valid for any kernels satisfying Hypothesis 1 and the examples are only here to illustrate the kind of kernel that could be used.

**3.1. Asymptotic Fokker-Planck Model Reduction.** To derive a reduced Fokker-Planck-like collision operator, we follow the strategy described in [12] for swarming models reminiscent of similar approaches used in granular media descriptions [8, 50], social phenomena such opinion dynamics [29, 51], and wealth distribution models [15]. This approach comes back to grazing collision limits in kinetic theory [18, 49]. Let us assume that except in the neighbourhood of  $\tilde{\phi} = 0$ , the orientation kernel  $\omega(\tilde{\phi}, \tilde{\theta})$  is negligible.

**Hypothesis 1.** For a small enough  $\varepsilon$  there exist two functions: a  $\frac{\pi}{\varepsilon}$ -periodic function  $g \in L^\infty\left(\left[-\frac{\pi}{2\varepsilon}, \frac{\pi}{2\varepsilon}\right]\right)$  and a  $\pi$ -periodic function  $h : \mathbb{R} \mapsto \left[-\frac{\pi}{2}, \frac{\pi}{2}\right]$  such that

- the orientation kernel satisfies the following scaling

$$\omega_\varepsilon(\tilde{\phi}, \tilde{\theta}) = g_\varepsilon(\tilde{\phi} - \varepsilon h(\tilde{\theta})) \quad \text{with} \quad g_\varepsilon(s) = \frac{1}{\varepsilon} g\left(\frac{s}{\varepsilon}\right).$$

- for any  $\tilde{\phi} \in [-\frac{\pi}{2}, -\varepsilon\frac{\pi}{2}] \cup [\varepsilon\frac{\pi}{2}, \frac{\pi}{2}]$  we have  $g_\varepsilon(\tilde{\phi}) = O(\varepsilon^3)$ .

This hypothesis mainly means that the fibres are unlikely to jump to distant orientations or influence very different orientations.

The periodicity assumptions on  $g$  and  $h$  provide that the orientation kernel  $\omega(\tilde{\phi}, \tilde{\theta})$  is  $\pi$ -periodic with respect to both variables. We note that  $g_\varepsilon$  equals to  $\bar{g}_\varepsilon$  from (3), extended by zero to  $[-\frac{\pi}{2\varepsilon}, \frac{\pi}{2\varepsilon}]$  satisfies the assumption for  $\varepsilon$  small enough. Moreover, the construction of other  $C^\infty$  functions satisfying the properties based on approximations of this finite angle reorientation region is relatively straightforward. An example of a simple functions  $h$  satisfying our assumptions is  $h(s) = \sin(2s)$ .

Now, we focus on the turning rate  $T$  given by (2). We rewrite the model in the weak form, and for simplicity we express the nonlinear weight  $\mu[f](t, y, \theta)$  as

$$\mu[f](t, y, \theta) = \frac{f(t, y, \theta)}{\rho(t, y)} \quad \text{with} \quad \rho(t, y) := \int_{-\frac{\pi}{2}}^{\frac{\pi}{2}} f(t, y, \theta') d\theta'.$$

Multiplying the collision operator by a  $\pi$ -periodic test function of the orientation  $\Psi \in L^2([-\frac{\pi}{2}, \frac{\pi}{2}])$  and integrating over the orientation, we obtain

$$\begin{aligned} \int_{-\frac{\pi}{2}}^{\frac{\pi}{2}} Q(f)\Psi(\phi) d\phi &= \int_{-\frac{\pi}{2}}^{\frac{\pi}{2}} \int_{-\frac{\pi}{2}}^{\frac{\pi}{2}} f(t, x, \phi) T(x, \phi, \phi') (\Psi(\phi') - \Psi(\phi)) d\phi' d\phi \\ &= \int_{\mathcal{D}} \int_{-\frac{\pi}{2}}^{\frac{\pi}{2}} \frac{f(t, y, \theta)}{\rho(t, y)} \kappa(x - y) \int_{-\frac{\pi}{2}}^{\frac{\pi}{2}} f(t, x, \phi) A(\phi, \theta) d\phi d\theta dy \end{aligned}$$

with

$$A(\phi, \theta) = \int_{-\frac{\pi}{2}}^{\frac{\pi}{2}} \omega(\phi - \phi', \phi - \theta) (\Psi(\phi') - \Psi(\phi)) d\phi'.$$

Then, using the Hypothesis 1 and the Taylor expansion, we get

$$\begin{aligned} A(\phi, \theta) &= \int_{\phi - \varepsilon h(\phi - \theta) - \varepsilon \frac{\pi}{2}}^{\phi - \varepsilon h(\phi - \theta) + \varepsilon \frac{\pi}{2}} g_\varepsilon(\phi - \phi' - \varepsilon h(\phi - \theta)) \cdot \\ &\quad \cdot \left( (\phi' - \phi) \Psi'(\phi) + \frac{(\phi' - \phi)^2}{2} \Psi''(\phi) \right) d\phi' + O(\varepsilon^3) = \\ &= G_1(\phi - \theta) \Psi'(\phi) + G_2(\phi - \theta) \Psi''(\phi) + O(\varepsilon^3), \end{aligned}$$

with the parameters

$$G_a(\tilde{\theta}) = \frac{\varepsilon^a}{a} \int_{-\frac{\pi}{2}}^{\frac{\pi}{2}} (\beta + h(\tilde{\theta}))^a g(\beta) d\beta, \quad \text{with} \quad a \in \{1, 2\}$$

and where we have set  $\beta = \frac{\phi - \phi'}{\varepsilon} - h(\phi - \theta)$ . Let us introduce the following coefficients

$$C[f](t, x, \phi) = \int_{-\frac{\pi}{2}}^{\frac{\pi}{2}} K[f](t, x, \theta) G_1(\phi - \theta) d\theta, \quad (5)$$

$$D[f](t, x, \phi) = \int_{-\frac{\pi}{2}}^{\frac{\pi}{2}} K[f](t, x, \theta) G_2(\phi - \theta) d\theta, \quad (6)$$

and

$$K[f](t, x, \theta) = \int_{\mathcal{D}} \frac{\kappa(x - y) f(t, y, \theta)}{\rho(t, y)} dy.$$

The collision operator can be approximated as

$$\begin{aligned} \int_{-\frac{\pi}{2}}^{\frac{\pi}{2}} Q(f) \Psi(\phi) d\phi &\simeq \\ &\simeq \int_{-\frac{\pi}{2}}^{\frac{\pi}{2}} (-C(t, x, \phi) \partial_{\phi} \Psi + D(t, x, \phi) \partial_{\phi}^2 \Psi) f(t, x, \phi) d\phi + O(\varepsilon^3). \end{aligned}$$

We can rewrite it in the classical formulation by integrating by parts to obtain a nonlinear non-local approximation of our integral operator by

$$Q(f) = \frac{\partial}{\partial \phi} \left( C[f](t, x, \phi) f + \frac{\partial}{\partial \phi} (D[f](t, x, \phi) f) \right) + O(\varepsilon^3)$$

Therefore, we can reduce the complexity of our model to the nonlinear non-local Fokker-Planck equation

$$\frac{\partial f}{\partial t}(t, x, \phi) = \frac{\partial}{\partial \phi} \left( C[f](t, x, \phi) f + \frac{\partial}{\partial \phi} (D[f](t, x, \phi) f) \right). \quad (7)$$

Notice that it is straightforward to check that a Dirac delta centred at a given orientation is a stationary weak solution of (7) in the particular case of both  $g$  and  $\kappa$  to be Dirac deltas at 0 as soon as  $h(0) = 0$ .

**4. Numerical approximation.** The following section consists of two parts. First, we provide necessary details on the numerical scheme developed to numerically approximate (7). Then we present the actual simulation results together with a discussion on the impact of particular parameters on observed dynamics. We conclude the subsection with considerations on the possible biological interpretation of the results.

**4.1. Numerical scheme.** To approximate the solution of the Fokker-Planck like model (7) we use a classical explicit Euler finite volume scheme with an upwind finite volume discretisation. To this end, we rewrite the model (7) in the form of a nonlinear continuity equation

$$\frac{\partial}{\partial t} f(t, x, \phi) + \frac{\partial}{\partial \phi} (f(t, x, \phi) U[f](t, x, \phi)) = 0, \quad (8)$$

where

$$U[f](t, x, \phi) := - \left( C[f] + \frac{\partial}{\partial \phi} D[f] + D[f] \frac{\partial}{\partial \phi} \log f \right) (t, x, \phi). \quad (9)$$

Consider a regular grid of  $N_x$  points in space and  $N_{\phi}$  points in orientation. Let  $\delta_x = \frac{|\mathcal{D}|}{N_x}$  and  $\delta_{\phi} = \frac{\pi}{N_{\phi}}$  be the space step and the orientation step, respectively, whereas the discrete time  $t^{n+1} = t^n + \delta_t^n$  with the time step  $\delta_t^n$  is defined by CFL condition (11). We denote the time index by  $n \in \mathbb{N}$ , the space index by  $k \in [0, N_x - 1] \cap \mathbb{N}$  and the orientation index by  $j \in [0, N_{\phi} - 1] \cap \mathbb{N}$ . Now  $f_{k,j}^n$



stands for an approximation of  $f(t^n, (k + 1/2)\delta_x, j\delta_\phi)$ . The explicit Euler scheme with an upwind finite volume discretisation of (8) reads as

$$f_{k,j}^{n+1} = f_{k,j}^n - \frac{\delta_t^n}{\delta_\phi} \left( f_{k,j}^n \left( \left( U_{k,j+1/2}^n \right)_+ + \left( U_{k,j-1/2}^n \right)_- \right) - f_{k,j+1}^n \left( U_{k,j+1/2}^n \right)_- - f_{k,j-1}^n \left( U_{k,j-1/2}^n \right)_+ \right), \quad (10)$$

where the positive and negative part functions were used, i.e.  $(\psi)_\pm = \frac{|\psi| \pm \psi}{2}$ . We define the approximation of the velocity  $U(n\delta_t^n, (k + 1/2)\delta_x, \phi)$  at the interface  $\phi = (j + 1/2)\delta_\phi$  by

$$U_{k,j+1/2}^n = - \left( C_{k,j+1/2}^n + \frac{D_{k,j+1}^n - D_{k,j}^n}{\delta_\phi} + D_{k,j+1/2}^n \frac{\log f_{k,j+1}^n - \log f_{k,j}^n}{\delta_\phi} \right).$$

For the convenience of the reader we recall that the numerical scheme is stable under a classical CFL condition. More precisely, for a fixed parameter  $0 < \lambda \leq 1$ , the time step is computed by

$$\delta_t^n = \frac{\lambda \delta_\phi}{\max_{j \in [1, N_\phi] \cap \mathbb{N}} \max_{k \in [1, N_x] \cap \mathbb{N}} \left( U_{k,j+1/2}^n \right)}, \quad (11)$$

we can then show the positivity of the numerical solution.

We propose the first-order numerical scheme for both orientation and time. We note that with the use of methods such as Monotonic Upstream-centred Scheme for Conservation Laws (MUSCL) or Weighted Essentially Non-Oscillatory scheme (WENO) for the discretisation of the orientation derivative and a Runge-Kutta scheme for time discretisation, it is possible to obtain higher accuracy. However, for our purposes, the proposed solution is sufficient. For more information on related finite volume discretisations, we refer the reader to papers [13, 11].

It remains for us to define the coefficients  $C_{k,j+1/2}^n$ , and  $D_{k,j+m/2}^n$  for  $m \in \{0, 1\}$ . Let us remark that the coefficients  $C$  and  $D$  are in fact convolution products in orientation between the functions  $G_i$  and the function  $K$ , and the latter is in fact a convolution product in space. The numerical integration was performed with a composite trapezium method, i.e. the discrete counterpart of

$$\int_0^1 A(x) dx \quad \text{is defined by} \quad \langle A_\star \rangle = \frac{1}{N} \left( \frac{A_0 + A_{N-1}}{2} + \sum_{j=1}^{N-2} A_j \right),$$

where  $A_i = A\left(\frac{i}{N-1}\right)$  for  $i \in [0, N-1] \cap \mathbb{N}$ . The discrete counterpart of the convolution product

$$\int_0^1 A(x) B(y-x) dx \quad \text{for } y = \frac{j}{N-1} \text{ yields} \quad [A_\star * B_\star]_j = \langle A_\star B_{j-\star_N} \rangle,$$

where  $\underline{n}_N = n - N \lfloor \frac{n}{N} \rfloor$  is the modulo operator and  $N$  stands for  $N_x$  or  $N_\phi + 1$  (because of the periodic bound) depending on whether we consider the space or the orientation convolution product. The star  $\star$  denotes the variable on which the convolution product acts in the case of several indexes.

The discrete counterparts of the operators  $C[f]$  from (5) and  $D[f]$  from (6) are defined as following

$$C_{k,j+1/2}^n = \pi [K_{k,\star}^n * G_{1,\star}]_{j+1/2} \quad \text{and} \quad D_{k,j+m/2}^n = \pi [K_{k,\star}^n * G_{2,\star}]_{j+m/2},$$

where  $m \in \{0, 1\}$ ,

$$K_{k,j}^n = |\mathcal{D}| \left[ \frac{f_{\star,j}^n}{\rho_{\star}^n} * \kappa_{\star} \right]_k \quad \text{with} \quad \kappa_k = \kappa(k\delta_x)$$

and coefficients  $G_{a,j+m/2}$  are the approximations of the functions  $G_a((j+m/2)\delta_\phi)$ .

For the  $\omega(\tilde{\theta}, \tilde{\phi})$  simple enough, it is possible to obtain analytically the function  $G_a(\tilde{\theta})$ , however for the general case of  $\omega(\tilde{\theta}, \tilde{\phi})$ , one can use the approximation

$$G_{a,j+m/2} = \frac{\varepsilon^a \pi}{a} \left\langle \tilde{G}_{\star}^{a,j+m/2} \right\rangle \quad \text{and} \\ \tilde{G}_i^{a,j+m/2} = \left( \left( i\delta_\phi - \frac{\pi}{2} \right) \right)^a g \left( \left( i\delta_\phi - \frac{\pi}{2} \right) - h((j+m/2)\delta_\phi) \right),$$

for  $j \in [0, N_\phi] \cap \mathbb{N}$  and  $i \in [0, N_\phi] \cap \mathbb{N}$ . Note, that these parameters are computed only once at the initial state and do not depend on the solution state. The density of the distribution  $f$  naturally reads  $\rho_k^n = \pi \left\langle f_{k,\star}^n \right\rangle$ .

**4.2. Computational simulation.** In this subsection, we present the results of the numerical simulation of the reduced Fokker-Planck type model (7). To present them in a clear way, we consider a 1D space domain  $\mathcal{D} = [0, 1]$ . We specify functions  $\kappa(\tilde{x}) = \kappa_R(\tilde{x})$  as defined by (3),  $g_\varepsilon(s) = \bar{g}_\varepsilon(s)$  as defined by (4), and finally we set  $h(\tilde{\theta}) = \sin(2\tilde{\theta})$ . The coefficient  $\kappa_0$  is fixed to 1, whereas the tenocyte action range  $R > 0$  and the reorientation range  $\varepsilon > 0$  varies in respective simulations, as we analyse their influence on the dynamics of the solution. As the initial condition, we take the function

$$f(0, x, \phi) = \frac{f^0(x, \phi)}{\int_{-\frac{\pi}{2}}^{\frac{\pi}{2}} f^0(x, \theta) d\theta},$$

where

$$f^0(x, \phi) = \sum_{i=1}^4 \exp \left( -\frac{\sigma_i^0}{x(1-x)} (\phi - A_i^0 \sin(\omega_i^0 x) \pi)^2 \right), \quad (12)$$

and parameters  $\sigma_i^0$ ,  $A_i^0$ , and  $\omega_i^0$  are given as

$i$	1	2	3	4
$\sigma_i^0$	10	10	5	20
$A_i^0$	0.1	0.2	-0.3	-0.15
$\omega_i^0$	$\pi$	$2\pi$	$3\pi$	$\pi$

For all the simulation, the time step is computed using the CFL condition (11) with the parameter  $\lambda = 1$ . These initial conditions are considered as a perturbation of a perfect vertically aligned fibres solution, that we can consider as the perfect healing solution.

In Figure 5 we show the time evolution of the solution to the numerical scheme presented in Subsection 4.1 obtained for three sets of parameters  $R$  and  $\varepsilon$  indicated at the top of each column, with the orientation and space resolutions set to  $N_\phi = 1000$  and  $N_x = 500$ . We first point out that we have run our simulations up to time  $t = 9$  at which we have achieved numerical equilibration in time. Our numerical simulations suggest as expected that the parameter  $\varepsilon$  locally impacts the time needed for reorientation. The global orientation (for all  $x$ ) is governed by the parameter  $R$ . For small  $R$  (column 1), the global orientation does not occur, or it is very slow (column 2). If  $R$  is large enough (column 3) the global vertical

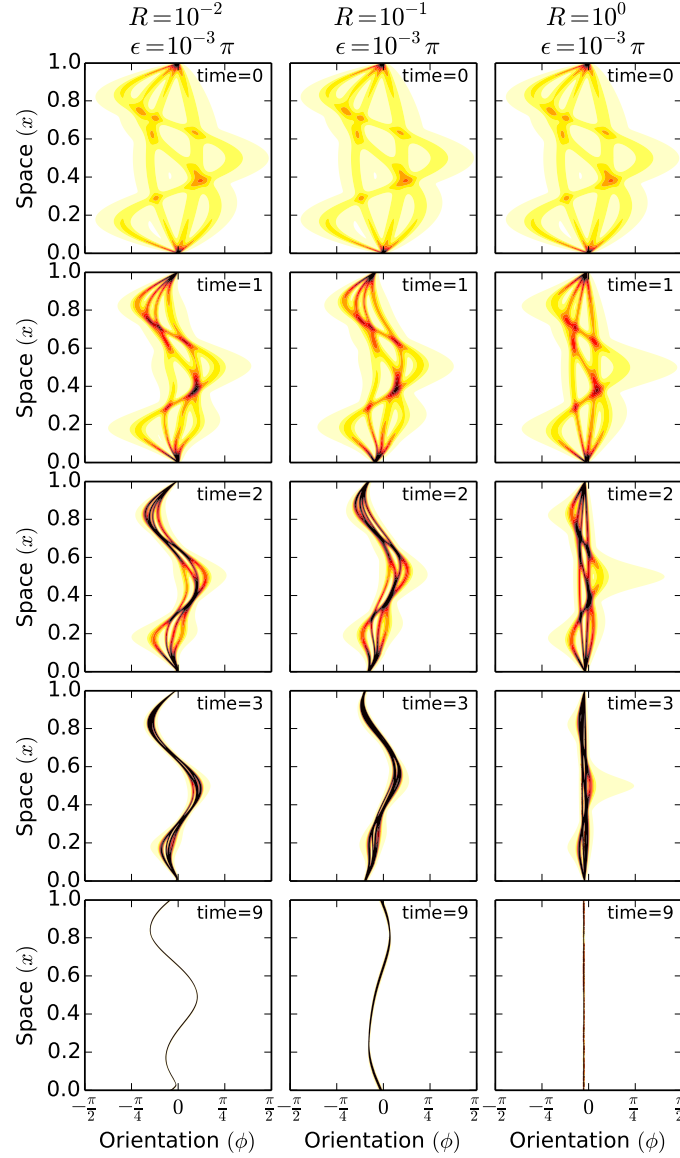


FIGURE 5. Time evolution of the solution to the model (7) performed for reorientation range  $\varepsilon = 10^{-3}\pi$  and different tenocyte action ranges  $R$  (value indicated at the top of each column). Colour scale represents the density value.

reorientation happens. Notice that in these simulations we have not fixed the values of the orientations at the bottom or the top in  $x$ . This can be easily adjusted in a more realistic tendon healing application since tendons at their ends are attached to the bones and muscles. We decided to leave the boundary conditions in  $x$  free to understand better the role of the parameters  $\varepsilon$  and  $R$ . Concerning the parameter  $\varepsilon \rightarrow 0$ , we observe that slow dynamics prevail and the steady state is only achieved

for very long times. The smallest value of  $\varepsilon$  for which our angular mesh  $N_\phi = 1000$  is fine enough is approximately  $10^{-2}\pi$ . In order to explore better the behaviour of the model for even smaller values of  $\varepsilon$ , a different more efficient numerical scheme has to be devised.

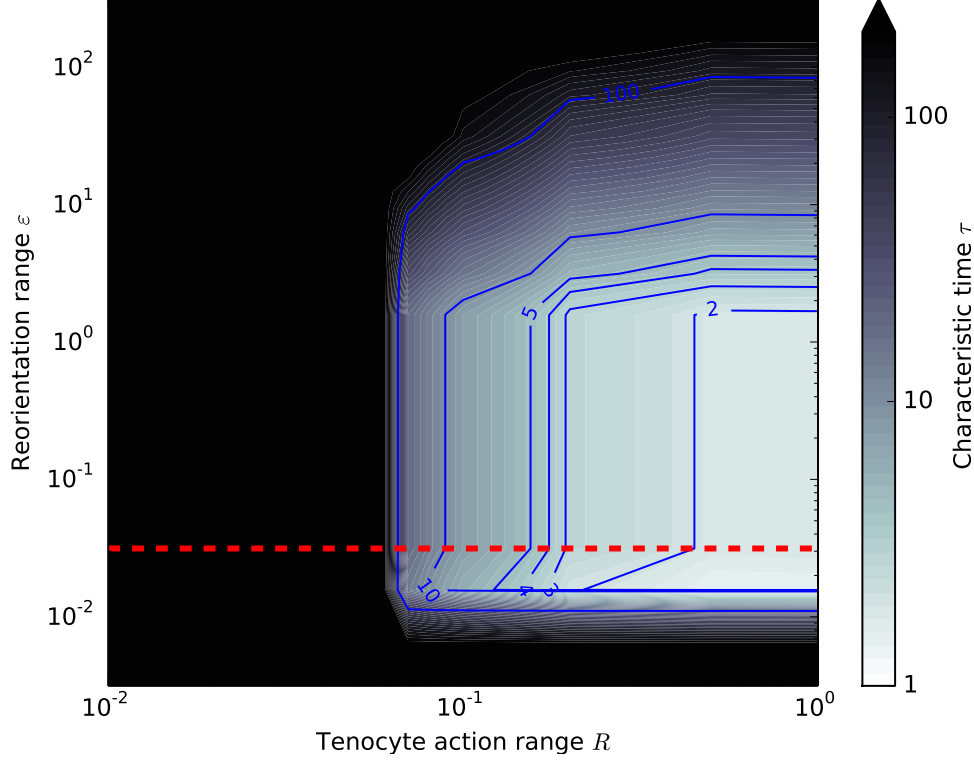


FIGURE 6. Characteristic time of the dynamic  $\tau$  as a function of the tenocyte action range  $R$  and reorientation range  $\varepsilon$  (log scale). The dashed red line indicates the minimum value for epsilon for the orientation resolution to be fine enough.

To assess more precisely the impact of parameters  $R$  and  $\varepsilon$  for the dynamics of the model, we have run a set of 300 simulations (with  $N_\phi = N_x = 300$ ) with the same initial condition (12), for large sets of tenocyte action range  $R$  and reorientation range  $\varepsilon$ . We define  $\tau$  to be the time needed for the variance of  $f$  to become smaller than 10% of the variance of the initial distribution (12). Time  $\tau$  is defined such that for any  $n$  when  $t^n > \tau$ , we have  $V^n \leq 10^{-1}V^0$ , where

$$V^n = \pi \left\langle \left( \theta_\star - \bar{\theta}^n \right)^2 F_\star^n \right\rangle \quad \text{with} \quad \theta_j = j\delta_\phi - \frac{\pi}{2},$$

$$\bar{\theta}^n = \pi \langle \theta_\star F_\star^n \rangle, \quad \text{and} \quad F_j^n = |\mathcal{D}| \langle f_{\star,j}^n \rangle.$$

Figure 6 presents a map of the relationship between time  $\tau$  and values of parameters  $R$  and  $\varepsilon$  created based on the 300 simulations conducted. We observe that as the parameter  $R$  decreases to 0, time  $\tau$  tends to infinity. The largest meaningful value for the parameter  $\varepsilon$  in terms of modelling is the size of the orientation domain  $\pi$ . As  $\varepsilon$  decreases the local reorientation gets slower, and when  $\varepsilon$  is smaller than

approximately  $10^{-2}\pi$ , i.e. below the dashed line in Figure 6, our results are not reliable since the mesh is too coarse. As mentioned above, exploring this range of parameters would need another numerical scheme to be developed.

From a biological perspective, by choosing function (12) as the initial condition, we intended to get, within the 1D framework, a simple representation of a tendon after surgical reconstruction and at the end of the proliferative stage of healing, when the rearrangement of fibres begins. The purpose of performing numerical simulations was to identify the parameters that actually influence the dynamics of the solution, and consequently to identify factors that might be important for the dynamics of tendon healing. The obtained results suggest that the range of spatial interactions influences the dynamics dramatically whereas, the size of the orientation kernel does not have a major impact on the result. Assuming that the range of spatial interactions is related to the size of the tenocytes, and not forgetting other crucial factors such as the rate of collagen synthesis, we hypothesise that the size of tenocytes plays an important role in the course of tendon healing. This could explain, at least in part, the importance of physical exercises for patient recovery. It is known from clinical practice that proper rehabilitation exercises are crucial for the healing process, however, it is not entirely clear why. A possible explanation is that the physical load affects the shape and size of the tenocytes. Without prejudging whether this working hypothesis is true, it is an important research topic for further investigation.

**5. Conclusions.** Tendon injuries give rise to significant morbidity, and at present only limited scientifically proven management modalities exist. A better understanding of tendon function and healing will allow specific treatment strategies to be developed. However, considering the complexity and multistage character of the tendon healing, a sensible strategy is to develop partial models of examined processes at first. Therefore, we restrict our attention to the latter stage of the healing process that consists mainly of the reconstruction of the parallel structure of collagen bundles mediated by tenocytes. The size of tenocytes, which is noticeable compared to the size of the collagen bundles, prompts us to capture their effect in non-local terms. Therefore we propose an integro-differential equation to describe the dynamics of the statistical density of collagen bundles distribution, with non-local terms standing for fibres' mutual influence. The proposed model contains two non-local kernels to capture the range of spatial and orientational influences. These two kernels require estimation before running the predictive simulations. Unfortunately, the numerical cost of the computation needed makes the estimation of the parameters with data assimilation tools very difficult. Therefore, we propose a model reduction that is suitable for this applications. Building in this approach and in related kinetic models for polymer flows [6, 7, 30], an interesting avenue of research could be to include elasticity effects through stress tensor coupling.

The result is the following working hypothesis that needs further investigation to ascertain biological relevance: tenocyte size is important for the tendon healing process. Moreover, we would like to emphasise the importance of model reduction. Nowadays, the majority of mathematical models, although interesting and providing a qualitative explanation of some phenomena, usually are missing a genuine connection to experimental data. The missing connection is particularly acute for models describing disease processes and response to treatment. Largely it is due to the difficulty of establishing proper experimental scenarios – which is precisely

the case of tendon healing. A solution may come with new advances in medical imaging. At present, these images do not have the resolution sufficient to obtain *in vivo* information on the arrangement of collagen fibres, however, progress is rapid. One can expect that high-grade data will soon become available allowing the inverse problem approach. Still, the inverse problem methodology requires huge computing resources. Considering these requirements the pertinent strategy may be an appropriate reduction of models, so as to simplify and shorten the numerical simulations while maintaining the essential features of the model.

**Acknowledgments.** J.A. Carrillo was supported the Advanced Grant Nonlocal-CPD (Nonlocal PDEs for Complex Particle Dynamics: Phase Transitions, Patterns and Synchronization) of the European Research Council Executive Agency (ERC) under the European Union’s Horizon 2020 research and innovation programme (grant agreement No. 883363). J.A. Carrillo was also partially supported by the EPSRC grant number EP/P031587/1. J.A. Carrillo and M. Parisot acknowledge the support from Institute of Mathematics, Polish Academy of Sciences within the framework “Małe spotkania badawcze”. Z. Szymańska was supported by the National Science Centre, Poland – grant No. 2017/26/M/ST1/00783. All medical image data were obtained within the National Centre for Research and Development grant STRATEGMED1/233224/10/NCBR/2014.

## REFERENCES

- [1] A. R. Akintunde and K. S. Miller, [Evaluation of microstructurally motivated constitutive models to describe age-dependent tendon healing](#), *Biomech Model Mechanobiol.*, **17** (2018), 793–814.
- [2] A. R. Akintunde, K. S. Miller and D. E. Schiavazzi, [Bayesian inference of constitutive model parameters from uncertain uniaxial experiments on murine tendons](#), *J Mech Behav Biomed Mater.*, **96** (2019), 285–300.
- [3] A. R. Akintunde, D. E. Schiavazzi and K. S. Miller, [Mathematical Model of Age-Specific Tendon Healing](#), *Computer Methods, Imaging and Visualization in Biomechanics and Biomedical Engineering*, Springer International Publishing, **36** (2020), 288–296.
- [4] J. Banasiak and M. Lachowicz, [Kinetic Model of Alignment](#), *Methods of Small Parameter in Mathematical Biology*, Modeling and Simulation in Science, Engineering and Technology, Birkhäuser, 2014.
- [5] P. K. Beredjikian, [Biologic Aspects of Flexor Tendon Laceration and Repair](#), *J Bone Joint Surg Am.*, **85** (2003), 539–550.
- [6] R. B. Bird, Ch. F. Curtiss, R. C. Armstrong and O. Hassager, Dynamics of polymeric liquids, *Volume 1: Fluid mechanics*, Wiley, (1987).
- [7] R. B. Bird, Ch. F. Curtiss, R. C. Armstrong and O. Hassager, Dynamics of polymeric liquids, *Volume 2: Kinetic Theory*, Wiley, (1987).
- [8] J. A. Carrillo, S. Cordier and G. Toscani, [Over-populated tails for conservative-in-the-mean inelastic Maxwell models](#), *Discrete Contin. Dyn. Syst. A.*, **24** (2009), 59–81.
- [9] J. A. Carrillo, M. Fornasier, J. Rosado and G. Toscani, [Asymptotic flocking dynamics for the kinetic Cucker-Smale model](#), *SIAM J. Math. Anal.*, **42** (2010), 218–236.
- [10] J. A. Carrillo and B. Yan, [An asymptotic preserving scheme for the diffusive limit of kinetic systems for chemotaxis](#), *Multiscale Model. Simul.*, **11** (2013), 336–361.
- [11] J. A. Carrillo, A. Chertock and Y. Huang, [A finite-volume method for nonlinear nonlocal equations with a gradient flow structure](#), *Commun Comput Phys.*, **17** (2015), 233–258.
- [12] J. A. Carrillo, R. Eftimie and F. Hoffmann, [Non-local kinetic and macroscopic models for self-organised animal aggregations](#), *Kinet. Relat. Models.*, **8** (2015), 413–441.
- [13] C. Chainais-Hillairet and F. Filbet, [Asymptotic behaviour of a finite-volume scheme for the transient drift-diffusion model](#), *IMA J. Numer. Anal.*, **27** (2007), 689–716.
- [14] A. Chauviere, L. Preziosi and T. Hillen, Modeling the motion of a cell population in the extracellular matrix, *Discrete Contin. Dyn. Syst. A.*, (2007), 250–259.

- [15] S. Cordier, L. Pareschi and G. Toscani, [On a kinetic model for a simple market economy](#), *J Stat Phys.*, **120** (2005), 253–277.
- [16] S. L. Curwin, [Rehabilitation after tendon injuries](#), *Tendon Injuries*, Springer-Verlag, **24** (2005), 242–266.
- [17] L. E. Dahners, [Growth and development of tendons](#), *Tendon Injuries*, Springer-Verlag, **3** (2005), 22–24.
- [18] P. Degond and B. Lucquin-Desreux, [The Fokker-Planck asymptotics of the Boltzmann collision operator in the Coulomb case](#), *Math. Models Methods Appl. Sci.*, **2** (1992), 167–182.
- [19] P. Degond and S. Motsch, [Continuum limit of self-driven particles with orientation interaction](#), *Math. Models Methods Appl. Sci.*, **18** (2008), 1193–1215.
- [20] D. Docheva, S.A. Müller, M. Majewski and H. E. Evans, [Biologics for tendon repair](#), *Adv. Drug Deliv. Rev.*, **84** (2015), 222–239.
- [21] M. Doumic, B. Perthame and J. P. Zubelli, [Numerical solution of an inverse problem in size-structured population dynamics](#), *Inverse Probl.*, **25** (2009), 045008, 25 pp.
- [22] M. Doumic, P. Maia and J. P. Zubelli, [On the calibration of a size-structured population model from experimental data](#), *Acta Biotheor.*, **58** (2010), 405–413.
- [23] M. Doumic, A. Marciniak-Czochra, B. Perthame and J. P. Zubelli, [A structured population model of cell differentiation](#), *SIAM J Appl Math.*, **71** (2011), 1918–1940.
- [24] M. Doumic, M. Hoffmann, N. Krell and L. Robert, [Statistical estimation of a growth-fragmentation model observed on a genealogical tree](#), *BERNOULLI*, **21** (2015), 1760–1799.
- [25] G. Dudziuk, M. Lachowicz, H. Leszczyński and Z. Szymańska, [A simple model of collagen remodeling](#), *Discrete Contin. Dyn. Syst. Ser. B.*, **24** (2019), 2205–2217.
- [26] R. Eftimie, G. de Vries and M. A. Lewis, [Complex spatial group patterns result from different animal communication mechanisms](#), *PNAS*, **104** (2007), 6974–6979.
- [27] R. C. Fetecau, [Collective behavior of biological aggregations in two dimensions: A nonlocal kinetic model](#), *Math. Models Methods Appl. Sci.*, **21** (2011), 1539–1569.
- [28] R. C. Fetecau and R. Eftimie, [An investigation of a nonlocal hyperbolic model for self-organization of biological groups](#), *J. Math. Biol.*, **61** (2009), 545–579.
- [29] G. Furioli, A. Pulvirenti, E. Terraneo and G. Toscani, [Fokker-Planck equations in the modeling of socio-economic phenomena](#), *Math. Models Methods Appl. Sci.*, **27** (2017), 115–158.
- [30] Y. Hyon, J. A. Carrillo, Q. Du and Ch. Liu, [A maximum entropy principle based closure method for macro-micro models of polymeric materials](#), *Kinet. Relat. Models.*, **1** (2008), 171–184.
- [31] G. Jull, A. Moore, D. Falla, J. Lewis, C. McCarthy and M. Sterling, *Grieve’s Modern Musculoskeletal Physiotherapy*, 4<sup>th</sup> ed., Elsevier, 2015.
- [32] D. Kader, M. Mosconi, F. Benazzo and N. Maffulli, [Achilles tendon rupture](#), *Tendon Injuries*, Springer-Verlag, **20** (2005), 187–200.
- [33] M. Kjær, Role of extracellular matrix in adaptation of tendon and skeletal muscle to mechanical loading, *Physiol. Rev.*, **84** (2004), 649–698.
- [34] M. Lachowicz, H. Leszczyński and M. Parisot, [Blow-up and global existence for a kinetic equation of swarm formation](#), *Math. Models Methods Appl. Sci.*, **27** (2017), 1153–1175.
- [35] H. Y. Li and Y. H. Hua, [Achilles tendinopathy: Current concepts about the basic science and clinical treatments](#), *Biomed Res Int.*, **2016** (2016), 6492597, 9 pp.
- [36] T. W. Lin, L. Cardenas and L. J. Soslowsky, [Biomechanics of tendon injury and repair](#), *J Biomech.*, **37** (2004), 865–877.
- [37] N. Loy and L. Preziosi, [Modelling physical limits of migration by a kinetic model with non-local sensing](#), *J Math Biol.*, **80** (2020), 1759–1801.
- [38] G. Nourissat, X. Houard, J. Sellam, D. Duprez and F. Berenbaum, [Use of autologous growth factors in aging tendon and chronic tendinopathy](#), *Front. Biosci.*, **E5** (2013), 911–921.
- [39] M. O’Brian, [Anatomy of tendon](#), *Tendon Injuries*, Springer-Verlag, **1** (2005), 3–13.
- [40] H. G. Othmer, S. R. Dunbar and W. Alt, [Models of dispersal in biological systems](#), *J Math Biol.*, **26** (1988), 263–298.
- [41] H. G. Othmer and T. Hillen, [The diffusion limit of transport equations. II. Chemotaxis equations](#), *SIAM J. Appl. Math.*, **62** (2002), 1222–1250.
- [42] M. Parisot and M. Lachowicz, [A kinetic model for the formation of swarms with nonlinear interactions](#), *Kinet. Relat. Models.*, **9** (2016), 131–164.
- [43] P. Sharma and N. Maffulli, Biology of tendon injury: Healing, modeling and remodeling, *J Musculoskelet Neuronal Interact.*, **6** (2006), 181–190.



- [44] P. Sharma and N. Maffulli, [Tendinopathy and tendon injury: The future](#), *Disabil Rehabil.*, **30** (2008), 1733–1745.
- [45] J. G. Snedeker and J. Foolen, [Tendon injury and repair - A perspective on the basic mechanisms of tendon disease and future clinical therapy](#), *Acta Biomater.*, **63** (2017), 18–36.
- [46] B. Perthame and J. P. Zubelli, [On the inverse problem for a size-structured population model](#), *Inverse Probl.*, **23** (2007), 1037–1052.
- [47] N. Takahashi, P. Tangkawattana, Y. Ootomo, T. Hirose, J. Minaguchi, H. Ueda, M. Yamada and K. Takehana, [Morphometric analysis of growing tenocytes in the superficial digital flexor tendon of piglets](#), *J Vet Med Sci.*, **79** (2017), 1960–1967.
- [48] C. T. Thorpe and H. R. C. Screen, [Tendon structure and composition](#), *Metabolic Influences on Risk for Tendon Disorders*, *Advances in Experimental Medicine and Biology*, Springer, **920** (2016), 3–10.
- [49] G. Toscani, [The grazing collisions asymptotics of the non-cut-off Kac equation](#), *Esaim Math Model Numer Anal.*, **32** (1998), 763–772.
- [50] G. Toscani, [One-dimensional kinetic models of granular flows](#), *Esaim Math Model Numer Anal.*, **34** (2000), 1277–1291.
- [51] G. Toscani, [Kinetic models of opinion formation](#), *Commun. Math. Sci.*, **4** (2006), 481–496.
- [52] F. Wu, M. Nerlich and D. Docheva, [Tendon injuries: Basic science and new repair proposals](#), *EFORT Open Rev.*, **2** (2017), 332–342.
- [53] G. Yang, B. B. Rothrauff and R. S. Tuan, [Tendon and ligament regeneration and repair: Clinical relevance and developmental paradigm](#), *Birth Defects Res. C, Embryo Today.*, **99** (2013), 203–222.
- [54] K. A. Young, J. A. Wise, P. DeSaix, D. H. Kruse, B. Poe, E. Johnson, J. E. Johnson, O. Korol, J. Gordon Betts and M. Womble, *Anatomy & Physiology*, OpenStax, 2013.

Received April 2020; 1st revision September 2020; final revision November 2020.

*E-mail address:* [carrillo@maths.ox.ac.uk](mailto:carrillo@maths.ox.ac.uk)

*E-mail address:* [martin.parisot@inria.fr](mailto:martin.parisot@inria.fr)

*E-mail address:* [z.szymanska@icm.edu.pl](mailto:z.szymanska@icm.edu.pl)